ELSEVIER

Carbohydrate Polymers 50 (2002) 407–415

Carbohydrate Polymers

www.elsevier.com/locate/carbpol

Dynamic rheology of agar gels: theory and experiments. Part II: gelation behavior of agar sols and fitting of a theoretical rheological model

K.C. Labropoulos[a], D.E. Niesz[a], S.C. Danforth[a,*], P.G. Kevrekidis[b]

[a]*Department of Ceramic and Materials Engineering, Rutgers University, 607 Taylor Road, Piscataway, NJ 08854-8065, USA*
[b]*Department of Mathematics and Statistics, University of Massachusetts, Lederle Graduate Research Tower, Amherst, MA 01003-4515, USA*

Received 26 November 2001; revised 7 March 2002; accepted 8 March 2002

Abstract

A theoretical rheological model for agar gels, based on the bead spring model for linear flexible random coils and the model for crosslinked polymers, is successfully fitted to experimental gelation curves obtained over a wide range of cooling rates (0.5–20 °C min^{-1}) and agar concentration (1–3 wt%). The theoretical gelation temperature, T_{gel}^{model} increases with increasing agar concentration and decreasing cooling rate. The intrinsic net association rate increases significantly with increasing cooling rate. This increase is related to the higher probability of association of the non-associated agar molecules at higher cooling rates.

Keywords: Dynamic rheology; Agar gel; Gelation behavior

1. Introduction

Agar gels form the basis for aqueous binder systems used in various powder consolidation methods such as powder injection molding (PIM) or gelcasting (Fanelli & Silvers; Fanelli, Silvers, Frei, Burlew, & Marsh, 1989; Behi, Fanelli, & Burlew; Olhero, Tarì, Coimbra, & Ferreira, 2000; Millán, Moreno, & Nieto, 2001; Olhero, Tarì, & Ferreira, 2001; Cesarano, 1989). Agar is a gel-forming polysaccharide extracted from seaweeds with a sugar skeleton consisting of alternating 1,3-linked β-D-galactopyranose and 1,4-linked 3,6 anhydro-α-L-galactopyranose units (Dea, McKinnon, & Rees, 1972; Arnott, Fulmer, Scott, Dea, Moorhouse, & Rees, 1974; Araki, 1956). The microstructural, mechanical and rheological properties of agar gels can be described by a 'crosslinked network' model (Dea et al., 1972; Arnott et al., 1974). In this model, a homogeneous aqueous sol is gradually changing to an elastic and turbid gel network during cooling. This transformation is reversible but path dependent (i.e. exhibits hysteresis).

The rheology of the gel phase plays an important role in the successful consolidation of ceramic or metal powders. The gelation behavior of agar sols is dependent on many factors including the agar concentration, the thermal history and the presence of additives. Nevertheless, to the best of our knowledge, no rheological model exists that can describe the rheological behavior of agar gels throughout the temperature range they are subjected to during consolidation (100–5 °C). In Part I of this study (Labropoulos, Niesz, Danforth, & Kevrekidids, 2002), the authors presented a rheological model to predict the evolution of the gel's dynamic moduli, utilizing concentration and time–temperature data. In Part II of this study, the gelation behavior of agar sols is examined as a function of agar concentration and cooling rate. The proposed theoretical model (Labropoulos et al., 2002) is then fitted to gelation curves covering a wide range of gelation conditions (1–3 wt% agar concentration and cooling rates of 0.5–20 °C min^{-1}). Information regarding certain model parameters such as the theoretical gelation temperature, T_{gel}^{model}, and the intrinsic association rate, $r(T)$, is obtained and useful conclusions can be drawn.

2. Theoretical background

A detailed discussion of the theoretical rheological model for agar gels was presented in Part I of this study (Labropoulos et al., 2002). The main features of the theoretical model are summarized below.

At high temperatures, agar molecules take on a random coil conformation. During cooling, agar molecules associate with each other forming double helices and higher order assemblies (suprafibers) (Dea et al., 1972; Arnott et al., 1974). The contributions from the non-associated molecules

* Corresponding author.
E-mail address: danforth@rci.rutgers.edu (S.C. Danforth).

0144-8617/02/$ - see front matter
PII: S0144-8617(02)00085-1

Table 1
Composition of agar gels

Material	Designation		
	AG1	AG2	AG3
Distilled and deionized and water (wt%)	99.0	98.0	97.0
Agar (wt%)	1.0	2.0	3.0

are theorized to be approximated by an adapted Rouse model, in which the monomeric friction coefficient, ζ_0, increases with decreasing temperature and accounts for the shift of the relaxation spectrum, τ_p, towards higher values: (Labropoulos et al., 2002)

$$\tau_p = \frac{\tau_1^{\text{ref}} T_{\text{ref}}}{p^2 T}\left(\frac{T_{\text{ref}} - T_{\text{low}}}{T - T_{\text{low}}}\right)^{A_2} \tag{1}$$

where τ_1^{ref} is the terminal relaxation time of the random coiled agar molecules at an arbitrary reference temperature T_{ref} (for example, $T_{\text{ref}} = 373.15$ K), T_{low} is a temperature that signifies the decreased mobility of the agar molecules as the freezing point is approached ($T_{\text{low}} = 273.15$ K), T is the absolute temperature (K) and A_2 is a power exponent that is related to the temperature dependence of $\zeta_0(T)$ (Labropoulos et al., 2002)

A theoretical gelation temperature, $T_{\text{gel}}^{\text{model}}$ is defined as the temperature at which a continuous three-dimensional network is formed for the first time. The gelation equation is approximated by the Verhulst equation, allowing an estimation of the number of associated molecules, n_{assoc}, as a function of agar concentration, time and temperature: (Labropoulos et al., 2002)

$$n_{\text{assoc}} = \frac{n_{\text{assoc}}^0 n_{\text{total}}}{n_{\text{assoc}}^0 + (n_{\text{total}} - n_{\text{assoc}}^0)\mathrm{e}^{-rt}} \qquad n_{\text{assoc}}^0 \le n \le n_{\text{total}} \tag{2}$$

$$r(T) = A_1 \underbrace{\left(\frac{T_{\text{ref}} - T_{\text{low}}}{T - T_{\text{low}}}\right)^{A_2}}_{\text{Mobility term}} \underbrace{\left(\frac{T_{\text{gel}} - T}{T_{\text{gel}} - T_{\text{low}}}\right)^{A_3}}_{\text{Driving force term}} \qquad T_{\text{low}} < T < T_{\text{gel}} \tag{3}$$

where n_{total} is the total number of agar molecules per unit volume, A_1, A_2 and A_3 are model parameters related to the net intrinsic association rate, $r(T)$, and T_{low} is the lower temperature limit of applicability of Eq. (3).

At temperatures below T_{gel} the rheological behavior of agar gel is dominated by contributions from an evolving agar network. The network contributions to the dynamic moduli of the system consist of frequency dependent (δ_{FSA}, δ_{FSB}, δ_{FVA}, δ_{FVB}) and frequency independent terms ($G'|^{c,t,T}_{\text{NET FREQ INDP}}$ and $G''|^{c,t,T}_{\text{NET FREQ INDP}}$) (Labropoulos et al., 2002). The frequency dependence of the network gradually disappears as more and more agar molecules associate and increase the stiffness of the network. The reader is directed to Part I of this study for a detailed discussion of the model and the physical significance of the model parameters (Labropoulos et al., 2002).

3. Experimental procedure

3.1. Materials

The powdered agar (agar agar NF Type S-100 PC 11-2-122-0) was provided by Frutarom Meer Corp., North Bergen, NJ. The total ash and acid insoluble ash were less

Table 2
Typical values of the model parameter used in fitting the proposed model to gelation curves of 1–3 wt% agar gels over a wide range of cooling rates

Cooling rate (°C min^{-1})	Agar concentration (wt%)	$T_{\text{gel}}^{\text{model}}$ (°C)	A_1	A_3	δ^*_{ISA}	δ_{SSB}	$\delta_{?\text{SB}}$	δ^*_{IVA}	δ_{SVB}	δ_{IVB}
0.5	1	43.9	0.132	1.59	−4	2	4.01	−4	1.5	2.52
	2	45.3	0.199	1.59	−8	2	3.91	−7	2	2.47
	3	46.0	0.214	1.59	−10	2	4.04	−5	2	2.42
1	1	43.4	0.134	1.33	−3	2	4.04	−4	1.5	2.42
	2	45.0	0.207	1.33	−6	2	4.00	−7	2	2.47
	3	45.6	0.238	1.33	−8	2	4.04	−5	2	2.34
5	1	38.4	0.750	1.12	−1	2	3.79	−4	1.5	2.60
	2	41.0	0.833	1.12	−2	2	3.83	−5	2	2.55
	3	42.7	0.864	1.12	−4	2	4.09	−5	2	2.46
10	1	37.4	1	0.90	−1	2	3.89	−4	1.5	2.63
	2	40.9	1.117	0.90	−2	2	3.85	−5	2	2.59
	3	42.1	1.224	0.90	−2	2	3.98	−3	2	2.43
20	1	37.2	1.854	0.85	−1	2	3.76	−4	1.5	2.64
	2	39.8	1.854	0.85	−2	2	3.90	−5	2	2.63
	3	42.0	1.854	0.85	0	2	3.96	0	2	2.32

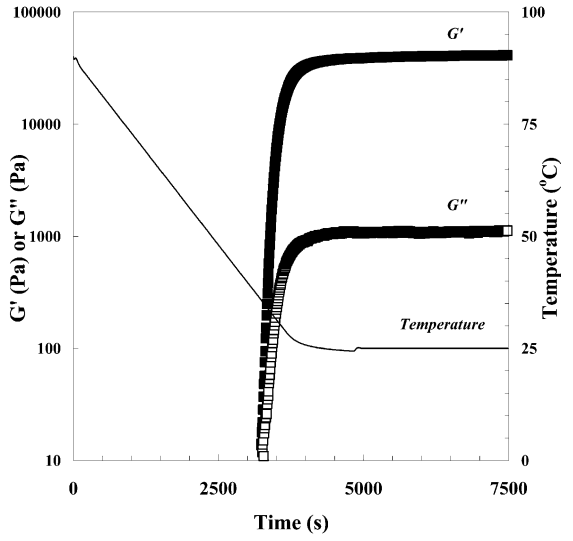

Fig. 1. Dynamic storage modulus, G' and dynamic viscous modulus, G'', vs. time of a 2 wt% agar gel on cooling from 90 to 25 °C at 1 °C at 1 °C min^{-1}. $t = 0$ at 90 °C during cooling, $\gamma = 1\%$, $\omega = 100$ rad s^{-1}, 25 mm parallel disk geometry.

than 6.5 and 0.5%, respectively. The agar powder had less than 20 wt% absorbed water (dried at 105 °C for 5 h). Agar sols were prepared by dissolving the powder in boiling, deionized and distilled water (pH = 6.5). The heated sol was held at 100 °C for 3 h and was continually stirred. The sample preparation procedure ensured that no water losses occurred. The sol was subsequently allowed to cool to room temperature inside the sealed reaction vessel. The compositions studied are listed in Table 1.

3.2. Dynamic rheology

Dynamic rheological measurements were performed on an advanced rheometric expansion system (ARES) controlled strain dynamic rheometer (Rheometric Scientific Inc. Piscataway, NJ) using a parallel plate geometry. Heating and cooling of the samples was achieved by a forced convection environmental chamber (oven). During testing at or above ambient temperature, air passed through resistive heaters in the oven. For very high cooling rates, evaporated liquid nitrogen supplied by an external cryogenic LN_2 controller was fed in the environmental chamber instead. The relatively small tool mass of the parallel plate geometry allowed relatively fast cooling rates to be attained (up to 20 °C min^{-1}).

Strain sweep experiments at the highest attainable frequency ($\omega = 100$ rad s^{-1}) and at various temperatures were performed in order to determine the linear viscoelastic region (LVER) of the gels. The LVER becomes narrower at higher frequencies and at higher temperatures. A strain, γ, of 1%, which fell within LVER (typically <5%), was selected to be used throughout the dynamic measurements for all compositions and temperatures. The selection of a strain value of such a low magnitude eliminated the slippage of the gel during measurement (Lai & Lii, 1997) and ensured a minimal influence of the shear field on the formation of the gel network (Norton, Jarvis, & Foster, 1999).

Temperature ramp experiments were used to study the gelation and liquefaction kinetics of the agar gels. Each sample was loaded at 25 °C and then heated to 95 °C to fully melt the gel. After 3 min above 90 °C, the sample was cooled to various temperatures at various cooling rates.

3.3. Results and discussion

3.3.1. Gelation kinetics

The typical gelation behavior of agar sols is shown in Fig. 1. The dynamic storage modulus, G', and the dynamic viscous modulus, G'', of a 2 wt% agar sol are plotted against time on cooling from 90 to 25 °C at a cooling rate of 1 °C min^{-1}. Reference time, t_0, was set to zero when the temperature reached 90 °C during cooling from 95 °C. Data below 10 Pa correspond to torque values below the resolution of the rheometer and are not shown. An abrupt increase in G' and G'' is observed at a temperature, T_{onset}, of approximately 35.7 ± 0.3 °C, indicating the initial formation of an elastic network ($G' > G''$). The moduli continue to increase even after the holding temperature has been reached. Eventually, they reach their equilibrium values of approximately 4.5×10^4 and 10^3 Pa, respectively.

The effect of agar concentration on the gelation behavior of agar sols is shown in Figs. 2 and 3, where the dynamic storage modulus, G', of 1–3 wt% agar sols is plotted vs. time and temperature, respectively, during cooling from 90 to 25 °C at 1 °C min^{-1}. The values of the equilibrium storage modulus, G'_e, for 1, 2 and 3 wt% agar sols are

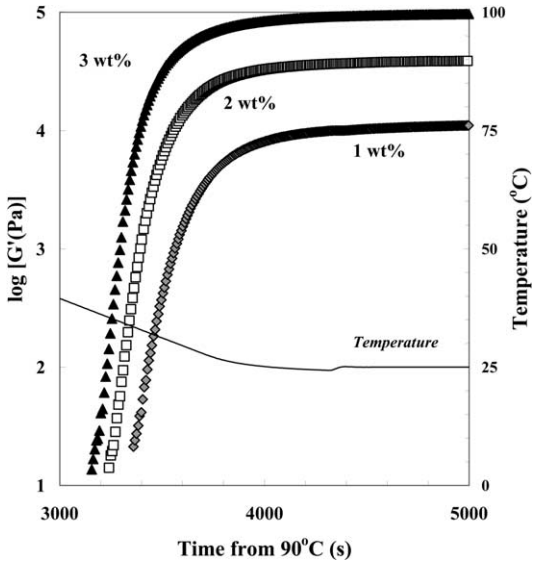

Fig. 2. Dynamic storage modulus, G', vs. time showing gelation behavior of agar gels (1–3 wt% agar) on cooling from 90 to 25 °C at 1 °C min^{-1}. $t = 0$ at 90 °C during cooling, $\gamma = 1\%$, $\omega = 100$ rad s^{-1}, 25 mm parallel disk geometry.

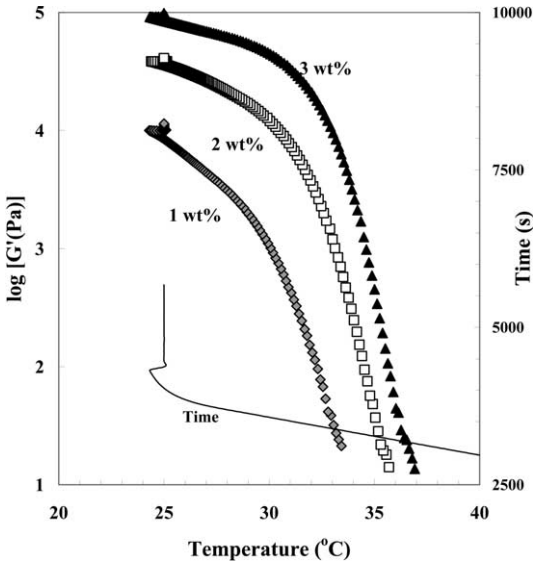

Fig. 3. Dynamic storage modulus, G', vs. temperature showing gelation behavior of agar gels (1–3 wt% agar) on cooling from 90 to 25 °C at 1 °C min^{-1}. $\gamma = 1\%$, $\omega = 100$ rad s^{-1}, 25 mm parallel disk geometry.

approximately 10^4, 4.5×10^4 and 10^5 Pa, respectively. These values are in good agreement with a c^2 dependence for agar concentrations above 1 wt% (where c is the agar concentration) (Mohammed, Hember, Richardson, & Morris, 1998; Lapasin & Pricl, 1995; Normand, Lootens, Amici, Plucknett, & Aymard, 2000; Ramzi, Rochas, & Guenet, 1998).

Fig. 2 indicates that gelation occurs sooner with increasing agar concentration. This is attributed to the higher probability of association when more agar molecules are present that results in the formation of a network earlier in the cooling process. Under the same cooling conditions, the onset of gelation, T_{onset} (and obviously T_{gel}), shifts to higher temperatures with increasing agar concentration. Fig. 3 shows that at a cooling rate of 1 °C min^{-1}, T_{onset} ranges from 34 to 37 °C.

Often the storage and viscous moduli drop to lower equilibrium values after reaching their maximum values. This phenomenon is probably associated with relaxation processes of the gel network. The phenomenon has also been attributed to a synergetic behavior or to the formation of superstrands in the gel network (Lai, Huang, & Lii, 1999). In this study, such relaxation processes are not included in the theoretical predictions. Instead, during fitting, we considered the maximum values of G' as the values for the equilibrium storage moduli for each gel composition.

In order to maximize the cycle time of PIM, the part will be held inside the cooled mold for the minimum time needed to allow gelation proceed to such a degree to allow handling of the molded part. Therefore, such relaxation processes after attaining the maximum moduli values may not be relevant, at least for the molding process. They may still play an important role during subsequent processes, including handling and drying.

The effect of cooling rate on the gelation behavior of agar sols is illustrated in Fig. 4 for a 2 wt% agar sol cooled at various cooling rates (from 0.5 to 20 °C min^{-1}) from 90 to 10 °C. It should be mentioned that since cooling of the tools and gel was accomplished by cold air through the forced convection oven, the cooling rate decreased as temperature approached ambient conditions. Therefore, the effective or average cooling rate until the onset of gelation was smaller than the commanded one. This was more pronounced for the fast cooling rates (with air). To solve this problem, evaporated liquid nitrogen was used for cooling rates higher than 1 °C min^{-1}. This allowed a constant cooling rate down to low temperatures. The forced convention oven was deactivated at 10 °C to prevent overshooting of the temperature to below zero.

The decrease of the cooling rate as temperature approaches the holding point (in this case ambient conditions) is a behavior that is also expected to occur in PIM. The cooling rate is reduced as the difference between the temperature of the molded material and the temperature of the cooled mold is decreased.

Fig. 4 indicates that the onset of gelation occurs at lower temperatures with increasing cooling rate. This has been reported in the literature (Harris, 1990) and is probably attributed to the reduced stiffness of the network formed under rapid cooling conditions compared to slower cooling patterns. As the cooling rate increases, the molecules associate in a more random way and do not have time to form equilibrium structures (such as closed packed stiff suprafibers) before their mobility is decreased (either due to physical hindrance or due to the low temperature). Gels formed

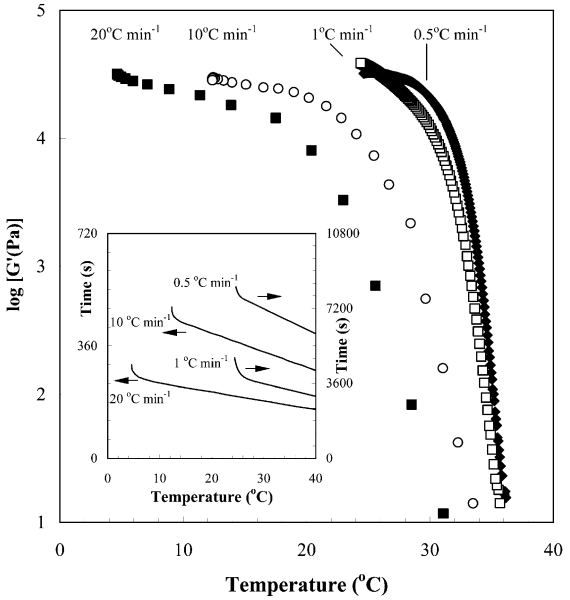

Fig. 4. Dynamic storage modulus, G', vs. temperature showing gelation behavior of a 2 wt% agar gel (on cooling from 90 to 25 °C at the indicated cooling rates (inset plot: 10 and 20 °C min^{-1} cooling rates use the left time axis, 0.5 and 1 °C min^{-1} cooling rates use the right time axis). $\gamma = 1\%$, $\omega = 100$ rad s^{-1}, 25 mm parallel disk geometry.

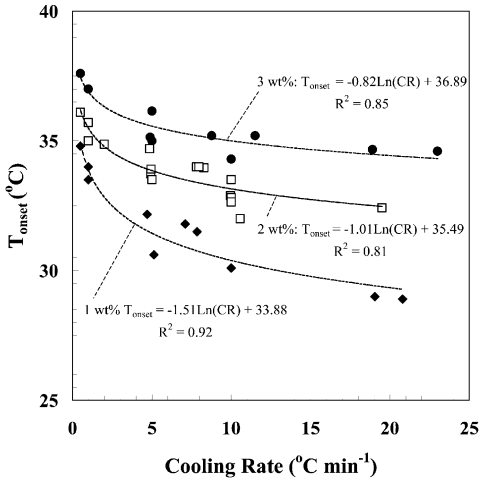

Fig. 5. Variation of the onset temperature for network formation, T_{onset} with cooling rate and agar concentration. The cooling rate is calculated from the time needed to cool from 90 °C to T_{onset}. $\gamma = 1\%$, $\omega = 100$ rad s^{-1}, 25 mm parallel disk geometry.

by controlled slow cooling have higher values of equilibrium moduli compared to gels obtained by rapid quenching (Mohammed et al., 1998). This behavior was also observed in this study and as will be discussed later, the modeling parameters were adjusted accordingly. The enhancement in the equilibrium storage moduli values with slower cooling rates is probably related to the formation of longer and stiffer suprafibers (Mohammed et al., 1998) and the better packing efficiency of the double helices within the suprafibers.

Fig. 5 shows the variation of the onset temperature for network formation, T_{onset}, with agar concentration and cooling rate. The onset temperature decreases with decreasing agar concentration or higher cooling rates. Fig. 5 indicates that for each agar concentration, T_{onset} tends to a limiting value as the cooling rate is increased beyond 5 °C min^{-1}. This behavior was not verified for cooling rates higher than 20 °C min^{-1}, due to experimental difficulties. Therefore, it is not known if a further decrease of T_{onset}below the indicated plateau will occur at cooling rates higher than 20 °C min^{-1}.

The temperature of the onset of network formation, T_{onset} is related to the gelation temperature, T_{gel}. In general, $T_{onset} < T_{gel}$. In this study, we adopted the approach used by Mohammed et al. (1998) to estimate the gelation temperature, T_{gel}^{model}, that was used for modeling of the rheological behavior of agar gels.

In particular, 1–3 wt% agar sols were cooled from 90 to 25 °C at 0.5 °C min^{-1} and the values of the T_{onset}, as observed by a rapid increase in the value of G', were recorded. Then, for each agar concentration, agar sols were cooled from 90 °C to temperatures above the onset of gelation, and held at these temperatures for adequate time until gelation proceeded to an end.

Fig. 6 exhibits the gelation behavior of 2 wt% agar sols cooled from 90 °C at 0.5 °C min^{-1} and holding at temperatures of 36.5, 37.5, 39.0 and 41.5 °C. It is evident that the closer the holding temperature is to the gelation temperature, the slower the kinetics and hence the longer it takes to reach the equilibrium moduli values.

According to Mohammed et al. (1998) the time required for the samples to reach a set value of modulus (for example $G' = 1$ Pa) is related to the relative gelation rate at different temperatures. In this study, the resolution of the rheometer limited the minimum 'detectable' modulus value to approximately 10 Pa. Nonetheless, there was significant uncertainty in estimating the time to reach 10 Pa, especially for samples held at high temperatures. Instead, the time to reach 100 Pa during cooling from 45 °C, $t_{45C100P}$, was selected as a good measure of the onset of gelation. Specifically, the inverse of $t_{45C100P}$ was indicative of the gelation rate.

The reference temperature $T_{ref}^{hold} = 45\ ^{\circ}C$, was the same as in the study of Mohammed et al. (1998). The fact that T_{ref}^{hold} was very close to the $T_{onset}^{kinetic}$ for the 3 wt% agar sols did not pose a significant problem. If a higher reference temperature was selected (for example $T_{ref}^{hold} = 50$ °C) this should increase the holding times, $t_{50C100P}$ by 10 min compared to $t_{45C100P}$. This would be barely noticeable at high holding temperatures (for example, for the 3 wt% gel and a holding temperature, $T_{hold} = 45$ °C, $t_{45C100P}$ is approximately 10 h).

Fig. 7 shows the results of this analysis. The reciprocal of $t_{45C100P}$ decreases with increasing temperature (closer to the gelation temperature) extrapolating to zero (i.e. $T_{onset}^{kinetic}$) at approximately 42, 44 and 46 °C for 1, 2, and 3 wt% agar sols, respectively. The values of $T_{onset}^{kinetic}$ for each agar concentration were used as the values of the theoretical gelation temperature, T_{gel}^{model}, as used in the proposed model (Labropoulos et al., 2002) for a cooling rate of 0.5 °C min^{-1}. Then, these values formed the basis for the

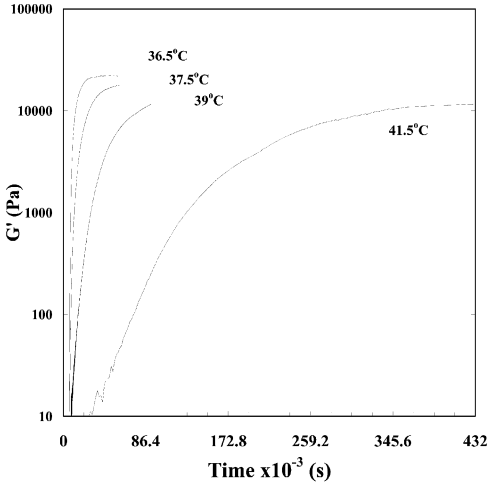

Fig. 6. Gelation curves (storage modulus, G', vs. time from 90 °C) of 2 wt% agar sols cooled from 90 °C at 0.5 °C min^{-1} and holding at temperatures of 36.5, 37.5, 39.0 and 41.0 °C. $\gamma = 1\%$, $\omega = 100$ rad s^{-1}, 25 mm parallel disk geometry.

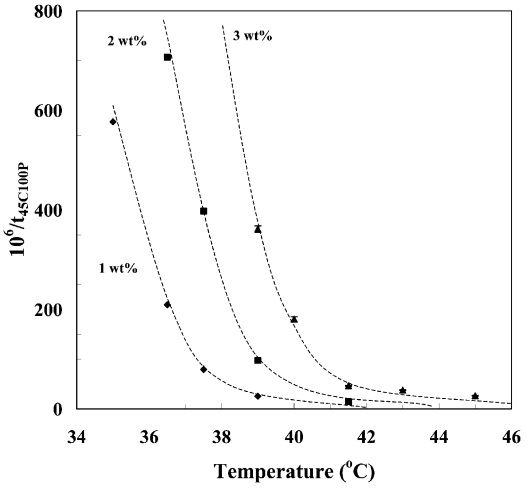

Fig. 7. Reciprocal relationship between the time ($t_{45C100P}$) needed for 1–3 wt% agar sols to reach 100 Pa during cooling from 45 °C at 0.5 °C min^{-1} and holding at the indicated temperature. Extrapolation of the curves (manual fitting) to $t_{45C100P} = \infty$ yields a $T_{onset}^{kinetic}$ of approximately 42, 44 and 46 °C for 1, 2 and 3 wt% agar sols, respectively.

evaluation of the T_{gel}^{model} at higher cooling rates, assuming a similar behavior as that indicated in Fig. 5.

3.3.2. Estimation of model parameters

These results indicate a rather strong dependence of the kinetics of the molecular association on the thermal history of the gels. However, a detailed investigation on the effect of the cooling rate on each model parameter was not the focus of this study. By keeping many of the parameters constant with values such that they satisfy a wide range of cooling conditions and agar concentrations, the proposed model could be validated and reveal the behavior of a few selected important parameters.

As discussed above, due to the measurement geometry, moduli values typically below 10 Pa, corresponded to torque values below the instrument resolution. Consequently, these data were assumed to have limited accuracy. This limited the range of the time–temperature domain over which the model could be fitted and allow the estimation of the model parameters.

Nevertheless, certain model parameters could be estimated by available information in the literature. Specifically, the terminal relaxation time, τ_1^{ref}, at the selected reference temperature $T_{ref} = 373.15$ K, was estimated using the following equation, which was assumed to be applicable even at such high temperatures (Rouse, 1953; Ferry, 1980):

$$\tau_1^{ref} = \frac{6[\eta]\eta_s M}{\pi^2 RT} \quad (4)$$

where $[\eta]$ is the intrinsic viscosity of the sol, M is the average molecular weight of the polymer and η_s is the viscosity of the solvent. Marinho-Soriano et al. reported an intrinsic viscosity for agar extracted from the species *Gracilaria bursa-pastoris* of approximately 500 ml g^{-1} at 25 °C (Marinho-Soriano, Bourret, Casabianca, & Maury, 1999). Lai and Lii reported intrinsic viscosity values for various agar fractions on the order of 100–200 ml g^{-1} at 45 °C (Lai & Lii, 1997). Estimation of the τ_1^{ref} using Eq. (4) yields a value in the order of 10^{-4}–10^{-5} s. A value of $\tau_1^{ref} = 10^{-4}$ s was subsequently used for all gels.

The critical concentration, c_0, below which no continuous gel network can form, is typically in the order of 0.1 wt% (Lapasin & Pricl, 1995). This value was used to estimate the value of n_{assoc}^0, assuming an average molecular weight of 120,000.

Fig. 8 indicates that the frequency dependence of the network is significant only at the early stages of gelation and mainly for the viscous modulus. Specifically, Fig. 8

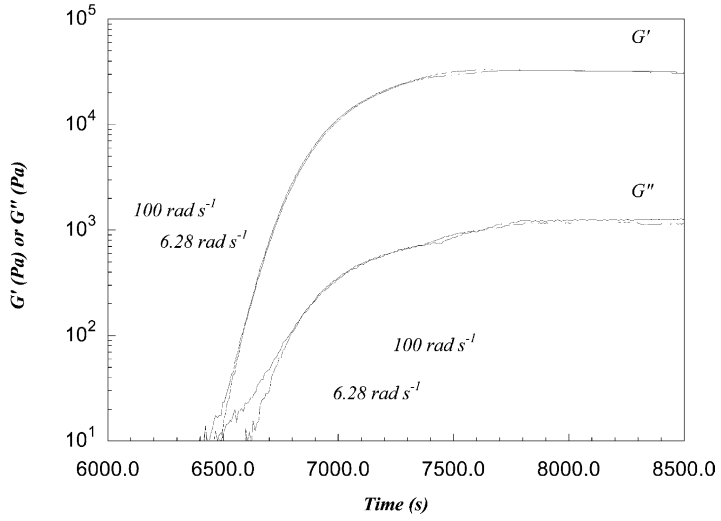

Fig. 8. Dynamic storage modulus, G', and dynamic viscous modulus, G'', of a 2 wt% agar sol as a function of time during cooling from 90 to 25 °C at 0.5 °C min^{-1}. The network that is gradually forming is dependent on frequency at the early stages of gelation, but becomes largely independent of frequency at later stages of gelation. $\gamma = 1\%$, 25 mm parallel disk geometry.

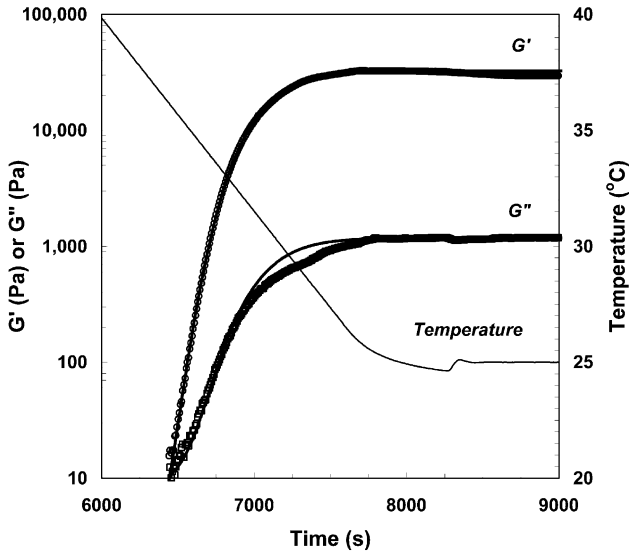

Fig. 9. Dynamic storage modulus, G' (open circles) and dynamic viscous modulus G'' (open squares) as a function of time for a 2 wt% agar sol cooled from 90 to 25 °C at 0.5 °C min^{-1}. Solid lines represent the theoretical predictions of the model using parameter values shown in Table 2. The theoretical predictions for G' and G'' are very close to the experimental data and the theoretical G'–G'' crossover matches the experimental one closely. $\gamma = 1\%$, $\omega = 100$ rad s^{-1}, 25 mm parallel disk geometry.

shows two different 2 wt% agar sols cooled from 90 to 25 °C at 0.5 °C min^{-1} and measured at two frequencies (6.28 and 100 rad s^{-1}, respectively). The values of the storage and viscous moduli at the early stages of gelation are dependent on frequency and in particular they decrease with decreasing frequency signifying a weak gel (Ferry, 1980). However, as gelation continues, the network moduli are largely independent of frequency signifying a strongly elastic gel (Ferry, 1980).

In order to simplify the study of the model, the functions δ_{FSA}, δ_{FSB}, δ_{FVA}, δ_{FVB} that describe the frequency dependence of the network were given the following empirical values for all agar concentrations and cooling conditions studied here: $\delta_{FSA} = \delta_{FSB} = \delta_{FVB} = 0.05$. The function δ_{FVA} varied with agar concentration taking values between 0.25 and 0.55 for 1–3 wt%, respectively. The frequency dependence of the network changes with time and temperature and is more complex than the above approximations, although its significance is greatly decreased during the later stages of gelation. Due to the lack of accurate data below approximately 10 Pa, the parameters describing the contributions from the *clusters* (δ_{FSM1}, δ_{FSM2}, δ_{FVM1}, δ_{FVM2}) were set to zero.

The remaining parameters were then varied accordingly to allow the model to be fitted as closely as possible to a number of gelation curves. Initially, fitting of the model was performed on gelation curves of sols cooled at 0.5 °C min^{-1}, using the gelation temperatures obtained from Fig. 7. Then the model was fitted to gelation curves from sols that were cooled at higher cooling rates (1 °C min^{-1} cooled with air, and 5, 10, 20 °C min^{-1} cooled with evaporated LN_2), assuming a cooling rate dependence of the gelation temperature similar to that of Fig. 5. The model parameters, A_1, c_{ABS}, c_{ABV}, δ^*_{ISA}, δ_{SSB}, δ_{ISB}, δ^*_{IVA}, δ_{SVB} and δ_{IVB} were adjusted empirically to allow the model to fit the data, minimizing the error between the theoretical predictions and the experimental values.

3.3.3. Results from fitting the model to gelation curves

The fitting effectiveness of the model within the range of cooling rates and agar concentrations studied here is illustrated in Fig. 9. Table 2 summarizes the set of the model parameters that were varied to fit the proposed model to gelation curves of 1–3 wt% agar sols cooled from 90 to 25 °C at a cooling rate ranging between 0.5 and 20 °C min^{-1}. Fig. 10 shows the dependence of the model parameter A_1 on agar concentration and cooling rate with the other model parameters as indicated in Table 2.

Fig. 9 shows that the proposed model can fit closely the gelation curve of a 2 wt% agar sol cooled at 0.5 °C min^{-1}. Similar results were obtained for other agar concentrations (1–3 wt%) and cooling rates (0.5–20 °C min^{-1}). Table 2 indicates that some of the model parameters (δ_{SSB}, δ_{ISB} and δ_{SVB}) remained rather constant, demonstrating the ability of the proposed model to fit the data satisfactorily with fewer fitting parameters. This is important when using agar powders different from the one used in this study. In such a case, it is expected that only a few gelation curves are needed (for example at two cooling rates and at two agar concentrations) to establish the magnitude of the model parameters.

The parameters A_2, c_{ABS}, c_{ABV}, *us*, and *uv* are not included in Table 2. The model could fit the data successfully by selecting c_{ABS} and c_{ABV} to be equal to the respective agar concentration, which simplified the analysis. The parameter A_2 was found to be rather constant for a wide range of agar

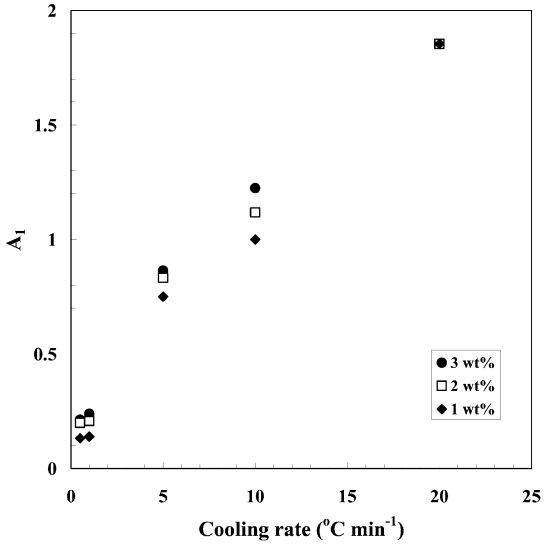

Fig. 10. Dependence of the model parameter A_1 on agar concentration and cooling rate and with all model parameters as indicated in Table 2.

concentrations and cooling rates; a value of $A_2 = 1.61$ was selected for all experiments. The parameters *us* and *uv* received empirical values of 1.8 and 1.6, respectively, for all experiments.

The presence of the above parameters in the equations of the proposed model allows flexibility in future studies over a wider range of cooling rates and agar concentrations. It can be observed (Table 2) that for each agar concentration and cooling rate, the theoretical gelation temperature, T_{gel}^{model}, is higher than the onset of network formation, T_{onset} (Fig. 5). In Part I of this study, it was pointed out that the onset of coil-to-helix transformation (i.e. $T_{onset}^{optical}$ as observed by the variation of the optical rotation) was occurring at higher temperatures compared to $T_{onset}^{modulus}$. The fact that T_{gel}^{model} is higher than the observed $T_{onset}^{modulus}$ is further supported by the set of experiments represented by Fig. 7, where sols held at temperatures above $T_{onset}^{modulus}$, but below the true gelation temperature of the sol (either T_{gel}^{model} or $T_{onset}^{optical}$), eventually gelled.

Table 2 indicates that T_{gel}^{model} increases with agar concentration.[1] This was expected if one compared Figs. 5 and 7. The cooling rate dependence of T_{gel}^{model}, however, was more complex. Fig. 5 indicated the possibility of a limiting value for T_{onset} (or at least a slow decrease of T_{onset} with cooling rate above approximately 5 °C min^{-1}). This could be extended to T_{gel}^{model}, so that the value of T_{gel}^{model} decreases with increasing cooling rate, up to approximately 5 °C min^{-1}. At higher cooling rates, T_{gel}^{model} remains largely constant. The results in Table 2 are based on this assumption.

Alternatively, T_{gel}^{model} can be decreased monotonically (i.e. there exists no plateau) with increasing cooling rate. Such an assumption affects mainly the parameter A_1. Typically, for a given agar concentration and cooling rate, if a higher T_{gel}^{model} was selected, the value of A_1 had to be decreased. Conversely, if a lower T_{gel}^{model} was selected, the value of A_1 had to be increased. These adjustments, however, resulted in worse fitting of the model to the experimental data, compared to the values of T_{gel}^{model} and A_1 in Table 2.

The values indicated in Table 2 are a set of parameters that allow satisfactory fitting of the model to the experimental data with all assumptions discussed above. Selection of different values of T_{gel}^{model} and subsequent adjustments of the remaining parameters may result in better fitting of the model to the experimental data, but that will probably involve adjustments to almost all of the model parameters. This approach, however, was beyond the scope of this study and will be attempted in future work.

Use of the proposed model for other types of agar powders will necessitate additional rheological measurements to evaluate the magnitude of the model parameters. It is preferable that a few sets of gelation curves are obtained at a very low cooling rate and at a high cooling rate. If one is not particularly interested at the rheological behavior at the onset of gelation (in which case the values of δ_{ISA}^{*} and δ_{IVA}^{*} can be obtained from Table 2), a few gelation curves (at least two concentrations and two cooling rates) should be able to provide the values of the parameters δ_{ISB} and δ_{IVB} and A_3 for other types of agars. The horizontal shifting (temperature axis) of the gelation curves of the new agars with respect to the gelation curves of the agar studied here, should provide an estimate of T_{gel}^{model} and A_1. The remaining parameters can take values described in this study, thus providing a satisfactory set of model parameters that allows use of the proposed model for other types of agars.

Fig. 10 indicates an approximately linear increase in the value of the parameter A_1 with increasing cooling rate. Effectively, a faster cooling rate increases the maximum value of the intrinsic association rate ($r(T)_{max} = A_1$). The increase of the maximum intrinsic association rate is probably related to the higher probability of random association with increasing cooling rate. Kusukawa, Ostrovsky, and Garner (1999) have studied the effect of cooling rate on the gel structure and resolving power of agarose sequencing gels. A comparison of transmission electron micrographs of a rapidly and slowly cooled 5.5% agarose gels revealed that the rapidly cooled gel resulted in a microstructure with thinner suprafibers and smaller pores. The slowly cooled agarose gels had a more heterogeneous structure (large open pores) and thicker fibers. The findings of the transmission electron micrographs were supported by optical density wavelength scans and calorimetric measurements during melting (differential scanning calorimetry, DSC). The same trend towards a microstructure with smaller pore sizes with increasing cooling rate was observed by Labropoulos (2001) for the type of agar used in this study.

It is theorized that the increase of A_1 with increasing cooling rate is associated with the different microstructural features of the evolving gel network under various cooling rates. In particular, one can visualize the case of a network (A) with short and thin suprafibers (and correspondingly small pore sizes) and another network (B), with the same total number of associated agar molecules, with long and thick suprafibers (and correspondingly large pore sizes). Network A is the result of high cooling rates, whereas network B is the result of slow cooling. It is apparent that the probability that a non-associated molecule will be attached to the network is higher for network A compared to network B. This example serves to explain the increase of A_1 (which is used in the equation for the intrinsic association rate and is related to the probability of association) with increasing cooling rate.

The dependence of the parameter A_1 on agar concentration is more complex. It seems that A_1 generally increases with agar concentration. Nevertheless, at increasing cooling rates the relative differences between the values of A_1 of different agar concentrations appear to be decreasing. In

[1] The increase of T_{gel}^{model} with agar concentration is probably real, since when T_{gel}^{model} was allowed to be independent of agar concentration, the gelation curves could not be fitted satisfactorily, even with appropriate adjustment of the remaining parameters.

fact, as indicated in Table 2, for the case of 20 °C min^{-1} cooling rate, a common value of A_1 could be used for the three agar concentrations studied.

The shape of the $\log G'|^{c,t,T}_{\text{NET FREQ INDP}}$ vs. $\log(c_{\text{app}})$ and $\log G''|^{c,t,T}_{\text{NET FREQ INDP}}$ vs. $\log(c_{\text{app}})$ curves (Labropoulos et al., 2002) is mainly affected by the parameters c_{ABS}, δ^*_{ISA}, *us*, δ_{SSB}, δ_{ISB} and c_{ABV}, δ^*_{IVA}, *uv*, δ_{SVB}, δ_{IVB}, respectively.[2] Table 2 indicates that the parameter δ^*_{ISA} tends to increase with cooling rate. Also, δ^*_{ISA} decreases at low cooling rates, with increasing agar concentration. The parameter δ^*_{ISA} was defined as the value of $\log G'|^{c,t,T}_{\text{NET FREQ INDP}}$ at $\log c_0$. Therefore, a value of $\delta^*_{\text{ISA}} = -10$ in the case of a 3 wt% agar gel cooled at 0.5 °C would indicate that $G'|^{c,t,T}_{\text{NET FREQ INDP}} = 10^{-10}$ Pa. This is an extremely low value for the initial gel network.

Instead, it is suggested that the low values of δ^*_{ISA} indicate high initial slopes of the $\log G'|^{c,t,T}_{\text{NET FREQ INDP}}$ vs. $\log c_{\text{app}}$ curve (i.e. the $y(x)$ function described in Labropoulos et al. (2002)) at $\log c_0$ (or equivalently x_0). The larger slope of $y(x)$ at x_0 (see Part I of this study) at higher agar concentrations means that the network attains its strength faster compared to lower concentrations. The apparent concentration dependence of $\log G'|^{c,t,T}_{\text{NET FREQ INDP}}$ becomes weaker at higher cooling rates, however, where δ^*_{ISA} tends to increase to a common large value. A similar discussion can be made for the parameter δ^*_{IVA} although there seems to be a weaker concentration and cooling rate dependence. The agar concentration and cooling rate dependence of the parameters δ_{SSB}, δ_{ISB}, δ_{SVB} and δ_{IVB} cannot be clarified within the statistical and experimental errors associated with the current variable analysis.

4. Conclusions

The proposed theoretical model was fitted successfully to a variety of gelation curves and provided useful information about important parameters related to the gelation kinetics ($T^{\text{model}}_{\text{gel}}$ and A_1). Sets of values for the remaining model parameters were provided in Table 2, which should form the basis for a more elaborate multivariate analysis in the future (including other types of agar powder, effect of substitutions in the basic agar chain and effect of molecular weight distribution on the model parameters). Even with this basic analysis, and having made several assumptions, the proposed model was able to fit the experimental data successfully, demonstrating a good flexibility of the model to fit to a wide range of thermal histories.

[2] Note that $T^{\text{model}}_{\text{gel}}$ and A_1 affect only how quickly the increase in $\log G'|^{c,t,T}_{\text{NET FREQ INDP}}$ or $\log G''|^{c,t,T}_{\text{NET FREQ INDP}}$ will occur as a function of $\log(c_{\text{app}})$.

Acknowledgements

This project was sponsored by the Malcolm G. McLaren Center for Ceramic Research, Rutgers University, and PowderFlow™ Technologies, Honeywell Int.

References

Araki, C. (1956). *Bulletin of Chemical Society of Japan*, *29*, 43.
Arnott, S., Fulmer, A., Scott, W. E., Dea, I. C. M., Moorhouse, R., & Rees, D. A. (1974). *Journal of Molecular Biology*, *90*, 269.
Behi, M., Fanelli, A. J., Burlew, J.V. (2000) *U.S. Patent*, 6, 146, 560.
Cesarano III, J. (1989). PhD Dissertation, University of Washington.
Dea, I. C. M., McKinnon, A. A., & Rees, D. A. (1972). *Journal of Molecular Biology*, *68*, 153.
Fanelli, A. J., Silvers, R. D. (1988) *U.S. Patent*, 4, 734, 237.
Fanelli, A. J., Silvers, R. D., Frei, W. S., Burlew, J. V., & Marsh, G. B. (1989). *Journal of American Ceramics Society*, *72*, 1833.
Ferry, J. D. (1980). *Viscoelastic properties of polymers*, (3rd ed). NY: Wiley.
Harris, P. (1990). *Food gels*, NY: Elsevier.
Kusukawa, N., Ostrovsky, M. V., & Garner, M. M. (1999). *Electrophoresis*, *20*, 1455.
Labropoulos, K. C., (2001). PhD Dissertation, Rutgers University.
Labropoulos, K. C., Niesz, D. E., Danforth, S. C., & Kevrekidids, P. G. (2002). *Carbohydrate Polymers*, this issue. Ref. Labropoulos: S0144-8617(02)00084-X.
Lai, M. -F., & Lii, C. (1997). *International Journal of Biological Macromolecules*, *21*, 123.
Lai, M. -F., Huang, A. -L., & Lii, C. (1999). *Food Hydrocolloids*, *13*, 409.
Lapasin, R., & Pricl, S. (1995). *Rheology of industrial polysaccharides: Theory and applications*, London, UK: Blackie A and P.
Marinho-Soriano, E., Bourret, E., de Casabianca, M. L., & Maury, L. (1999). *Bioresource Technology*, *67*, 1.
Millán, A. J., Moreno, R., & Nieto, M. I. (2001). *Material Letters*, *47*, 324.
Mohammed, Z. H., Hember, M. W. N., Richardson, R. K., & Morris, E. R. (1998). *Carbohydrate Polymers*, *36*, 15.
Normand, V., Lootens, D. L., Amici, E., Plucknett, K. P., & Aymard, P. (2000). *Biomacromolecules*, *1*, 730.
Norton, I. T., Jarvis, D. A., & Foster, T. J. (1999). *International Journal of Biological Macromolecules*, *26*, 255.
Olhero, S. M., Tarì, G., Coimbra, M. A., & Ferreira, J. M. F. (2000). *Journal of European Ceramics Society*, *20*, 423.
Olhero, S. M., Tarì, G., & Ferreira, J. M. F. (2001). *Journal of American Ceramics Society*, *84*, 719.
Ramzi, M., Rochas, C., & Guenet, J. -M. (1998). *Macromolecules*, *31*, 6106.
Rouse, P. E. (1953). *Journal of Chemical Physics*, *21*, 1272.